

Wavelet detection of singularities in the presence of fractal noise

Steven E. Noel, Yogesh Gohel, and Harold H. Szu
 Naval Surface Warfare Center Dahlgren Division, Dahlgren, VA 22448

ABSTRACT

Here we detect singularities with generalized quadrature processing using the recently developed Hermitian Hat wavelet. Our intended application is radar target detection for the optimal fuzing of ship self-defense munitions. We first develop a wavelet-based fractal noise model to represent sea clutter. We then investigate wavelet shrinkage as a way to reduce and smooth the noise before attempting wavelet detection. Finally, we use the complex phase of the Hermitian Hat wavelet to detect a simulated target singularity in the presence of our fractal noise.

Keywords: Hermitian Hat wavelet, radar quadrature processing, wavelet shrinkage, fractal noise.

1. INTRODUCTION

In this paper we generalize quadrature processing of radar signals using Szu's recently developed "Hermitian Hat" wavelet.¹ This complex-valued wavelet has an even function as its real part and an odd function as its imaginary part. These functions correspond to the cosine and sine in traditional quadrature processing. Like the complex exponential, the Hermitian Hat has no Fourier phase, so that the phase of the filter does not affect the phase of the signal. However, unlike the complex exponential, the Hermitian Hat is localized in time.

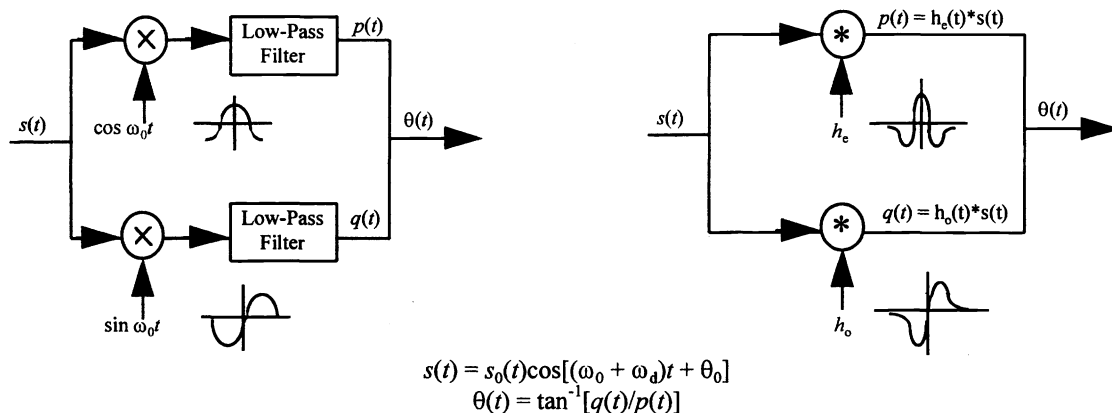


Figure 1. Traditional quadrature processing, and generalized quadrature processing with Hermitian Hat wavelet

With this generalized quadrature processing we wish to detect singularities representing radar returns from targets. Singularities are defined in terms of non-unique derivatives, but direct calculation of derivatives is inaccurate in the presence of noise. This is because the derivatives are undefined throughout the signal. However, techniques involving the complex phase of the Morlet wavelet have been successful in detecting singularities.² The sharpnesses of the singularities are revealed through bifurcations in the phase as the scale of the wavelet decreases.

Further author information -

S.E.N.: Email: snoel@nswc.navy.mil

Y.G.: Email: ygohel@nswc.navy.mil

H.H.S.: Email: hszu@nswc.navy.mil

Unfortunately, the Morlet wavelet has certain weaknesses. Its Fourier must vanish at zero, but the Morlet must oscillate at least 6 times within its Gaussian window to approximate this. This implies by the Nyquist theorem a relatively large number of necessary sample points. Also, being a relatively wide finite impulse response filter, it tends to smear the original singularity. The Hermitian Hat wavelet has the same phase bifurcation for singularity detection as the Morlet wavelet. However, it requires only about one and a half oscillations to have its Fourier transform nearly vanish at zero. It also exhibits less smearing than the Morlet.

We assume that the radar signal containing target singularities is corrupted by sea clutter noise. Since the ocean surface is fractal,³ we construct a model of sea clutter that is a variation of $1/f$ fractal noise. The model is wavelet-based, and relies on scale-dependent variances of the wavelet coefficients. We also assume that the signal-to-noise ratio is fairly low. Because of the relatively weak signal, the linear approach we take is appropriate.

At low signal-to-noise ratios, one may wish to first reduce and smooth the noise, thereby enhancing the signal to be detected. Donoho and Johnstone's wavelet shrinkage algorithm^{4,5,6,7,8} has proven to be very good at this. The algorithm is a form of nonparametric regression, in which the goal is to form an estimate of an unknown signal which has been corrupted by noise. The regression is nonparametric in the sense that minimal assumptions are made about the nature of the unknown function. The basic strategy of wavelet shrinkage is to apply the discrete wavelet transform, shrink a number of the wavelet coefficients towards zero in some fashion, then apply the inverse wavelet transform. It is based on the premise that the unknown signal is represented by relatively few wavelet coefficients, and that noise affects all coefficients, so that shrinking coefficients removes noise while preserving features.

In Naval operations, radar target detection in the presence of ocean surface noise is difficult. This is especially true in the case of ships defending themselves against sea-skimming cruise missiles. In our work, we are also particularly interested in the optimal fuzing of self-defense munitions to counter this threat. In the future the challenge of ship self-defense will only increase. This is because improved threats will be developed which skim lower, are faster, and which have reduced radar cross sections. The situation demands state-of-the-art signal processing algorithms such as wavelets. Their joint time/scale representation with a localized basis provides a great improvement over traditional Fourier methods for nonstationary signals. Also, Mallat's $O(n)$ pyramid algorithm⁹ provides an incredibly fast digital implementation.

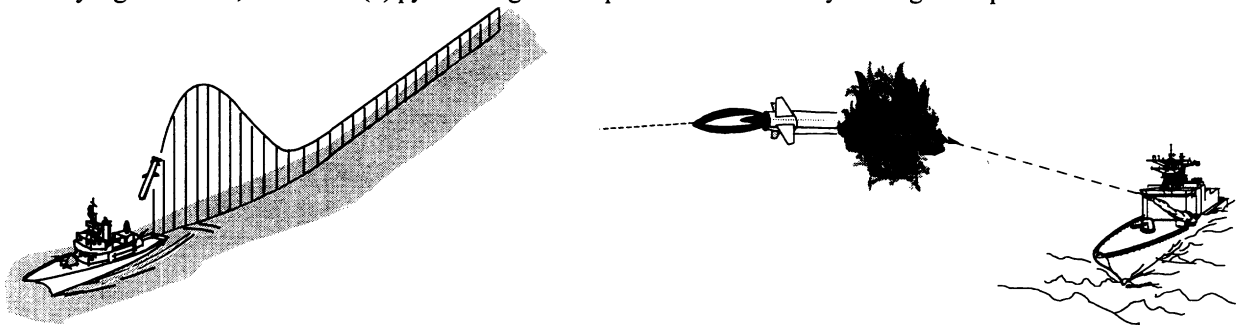


Figure 2. Ship self-defense against cruise missiles

2. WAVELET-BASED FRACTAL MODEL OF OCEAN SURFACE NOISE

As Mandelbrot pointed out, fractal behavior is the rule in nature.¹⁰ One fractal model which applies to a large number of natural phenomenon is so called $1/f$ noise.¹¹ These noises have power spectra as

$$S(\omega) = \sigma^2 / |\omega|^\gamma . \quad (1)$$

The spectra for $1/f$ noises obey a certain scaling equation for every scale a :

$$S(\omega) = |a|^\gamma S(a\omega) . \quad (2)$$

The noise statistics are therefore invariant to changes in scale, that is the noises are statistically self similar. This self similarity gives them a fractal structure. They also have long-term correlation, in that the autocorrelation $R(\tau)$ of their spectra decays as

$$R(\tau) = |\tau|^\gamma^{-1} . \quad (3)$$

The spectral parameter γ controls the degree of irregularity in the noise, and is related to the fractal dimension as $D = (5 - \gamma) / 2$. While this spectrum is not theoretically valid (it is non-integrable), many phenomena possess it over all measured frequencies.

Wavelet representations for $1/f$ noise have been developed¹² which are particularly useful in signal processing applications. Results have shown that nearly $1/f$ behavior can be generated from wavelet coefficients that are uncorrelated Gaussian noises with scale-dependent variances. Before we state this more precisely, recall that an orthonormal continuous wavelet transformation of a signal $x(t)$ is described as

$$x(t) = \sum_j \sum_k x_{j,k} \psi_{j,k}(t) \quad (4)$$

where the wavelet coefficients $x_{j,k}$ are

$$x_{j,k} = \int_{-\infty}^{\infty} x(t) \psi_{j,k}(t) dt. \quad (5)$$

The orthonormal basis functions $\psi_{j,k}$ are all dilations and translations of the mother wavelet ψ as

$$\psi_{j,k}(t) = 2^{-j/2} \psi\left(\frac{t - 2^j k}{2^j}\right). \quad (6)$$

A nearly $1/f$ noise is then constructed from the wavelet expansion (4) when the wavelet coefficients $x_{j,k}$ are uncorrelated zero-mean Gaussian random variables whose variances depend on their scale 2^j as

$$\text{var}(x_{j,k}) = \sigma^2 2^{j\gamma}. \quad (7)$$

The resulting random process is nearly $1/f$ in the sense that its time-averaged spectrum

$$S(\omega) = \sigma^2 \sum_j 2^{-j\gamma} |\Psi(2^j \omega)|^2 \quad (8)$$

is constrained as

$$\sigma_L^2 / |\omega|^\gamma \leq S(\omega) \leq \sigma_U^2 / |\omega|^\gamma. \quad (9)$$

Moreover, the resulting process has ripple which is octave spaced, that is for any integer k

$$|\omega|^\gamma S(\omega) = |2^k \omega|^\gamma S(2^k \omega). \quad (10)$$

Note that the wavelet basis is required to be R th-order regular where $R > \gamma/2$.

Mallat's multiresolution analysis⁹ allows us to interpret the wavelet decomposition as representing a signal at various resolutions (scales). It also leads to the very efficient pyramid algorithm for digital implementation. Multiresolution analysis gives a wavelet approximation of a continuous signal $x(t)$ in terms of orthogonal smooth and detail signal components

$$x(t) \approx S_J(t) + D_J(t) + D_{J-1} + \dots + D_1(t). \quad (11)$$

The smooth component S_J (at resolution 2^{-J}) and detail components D_j (at resolutions $2^{-j}, 2^{1-j}, \dots, 2$) are

$$S_J(t) = \sum_k s_{J,k} \phi_{J,k}(t) \quad (12a)$$

$$D_j(t) = \sum_k d_{j,k} \psi_{j,k}(t). \quad (12b)$$

It introduces scaling functions $\phi_{J,k}$ which are dilations and translations of the father wavelet ϕ , that is

$$\phi_{J,k}(t) = 2^{-J/2} \phi\left(\frac{t - 2^J k}{2^J}\right). \quad (13)$$

The scaling function coefficients $s_{J,k}$ are

$$s_{J,k} \approx \int x(t) \phi_{J,k}(t) dt. \quad (14)$$

We now apply multiresolution analysis to the construction of a fractal model for radar noise generated by the ocean surface. At spacial frequencies above some limit, we assume that the model has a $1/f$ spectrum. This seems reasonable since $1/f$ -type behavior is expected for higher frequencies, at least to the resolution limit of our measuring instruments. However, at lower spatial frequencies the ocean surface does not have a $1/f$ spectrum. For these lower frequencies (longer spatial

wavelengths) the wind is not powerful enough to generate waves which are tall enough to exhibit $1/f$ behavior. In other words, gravity limits the largest possible heights of waves. This is seen most dramatically when the ocean is viewed from space, in which it appears flat. Here we assume that the measurement length is large enough to actually observe non- $1/f$ behavior.

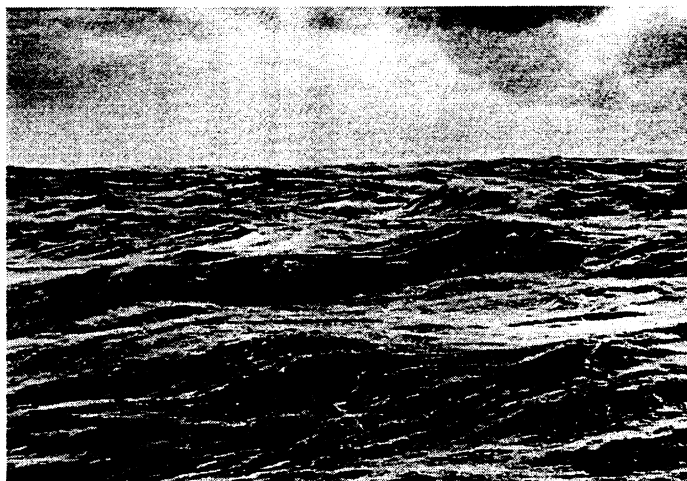


Figure 3. The ocean surface

We construct our noise model with a wavelet decomposition containing 6 scales. We choose the Daubechies s8 “symmlet” as the basis,¹³ shown in Figure 4. We apply the 2^{γ} variance condition in (7) to wavelet coefficients at all scales smaller than some limiting one, as consistent with $(1/f)$ behavior. At scales larger than the limiting one, we assume that variances become smaller as the scale increases, also in the manner of (7). Thus we choose variances for the detail coefficients $d_{j,k}$ as

$$\text{var}_j(d_{j,k}) = \begin{cases} 2^{j\gamma} & 1 \leq j \leq 4 \\ 2^{(8-j)\gamma} & 5 \leq j \leq 6. \end{cases} \quad (15)$$

For the smooth coefficients $s_{6,k}$ we choose

$$\text{var}(s_{6,k}) = 2^{\gamma}. \quad (16)$$

For all coefficient variances we choose the spectral parameter to be $\gamma = 1.5$.

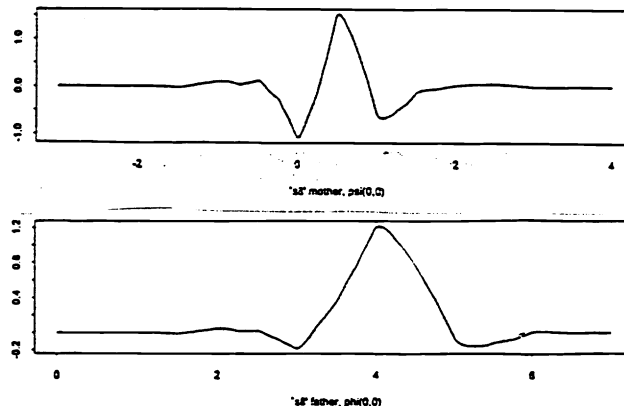


Figure 4. Daubechies s8 wavelet basis

The multiresolution decomposition and analysis for the resulting noise are shown in Figures 5 and 6. When seen on a more compressed horizontal scale, as in Figure 7, the synthesized fractal noise is surprisingly similar to actual radar measurements of sea clutter noise.¹⁴

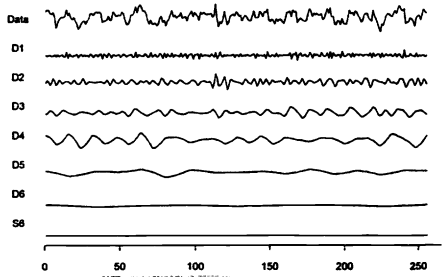


Figure 5. Multiresolution decomposition for fractal model of ocean surface noise

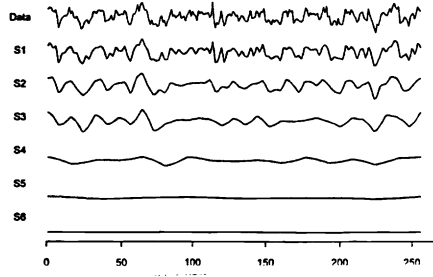


Figure 6. Multiresolution analysis for fractal model of ocean surface noise

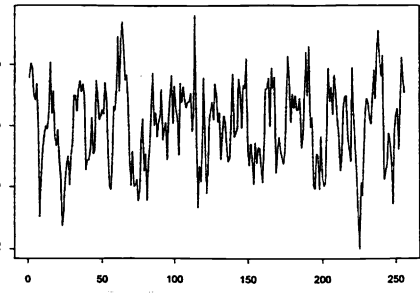


Figure 7. Fractal model of ocean surface noise

3. WAVELET SHRINKAGE FOR SINGULARITY ENHANCEMENT

Wavelet shrinkage is essentially a form of nonparametric regression. The goal is to form an estimate $\hat{x}(t)$ of an unknown signal $x(t)$ from noisy data samples x_i . We also wish to make minimal assumptions about the nature of x . The general approach is to apply the discrete wavelet transform to the noisy data, shrink a number of smaller scale wavelet coefficients towards zero, and apply the inverse transform. The idea is that noise affects all coefficients, so that shrinking them largely removes it. Since the unknown signal is represented by a relatively few number of coefficients, and those usually being at the larger scales, the signal features are generally preserved.

More precisely, the algorithm for wavelet shrinkage is to apply the discrete wavelet transform to some J scale levels, obtaining vectors of detail and smooth wavelet coefficients

$$\mathbf{d}_1, \mathbf{d}_2, \dots, \mathbf{d}_{J-1}, \mathbf{d}_J, \mathbf{s}_J. \quad (17)$$

We then shrink the detail coefficients at some $j < J$ smallest scales to obtain

$$\tilde{\mathbf{d}}_1, \tilde{\mathbf{d}}_2, \dots, \tilde{\mathbf{d}}_j \quad (18)$$

where

$$\tilde{\mathbf{d}}_j = \delta_{\lambda, \sigma_j}(\mathbf{d}_j). \quad (19)$$

Here $\delta_{\lambda, \sigma}(x)$ is a function which shrinks x towards zero, and is parameterized by a threshold λ and an estimate of the scale of the noise σ . Finally, we apply the inverse discrete wavelet transform using coefficients

$$\tilde{\mathbf{d}}_1, \dots, \tilde{\mathbf{d}}_j, \mathbf{d}_{j+1}, \dots, \mathbf{d}_J, \mathbf{s}_J \quad (20)$$

to obtain the wavelet shrinkage estimate. This algorithm is shown in Figure 8.

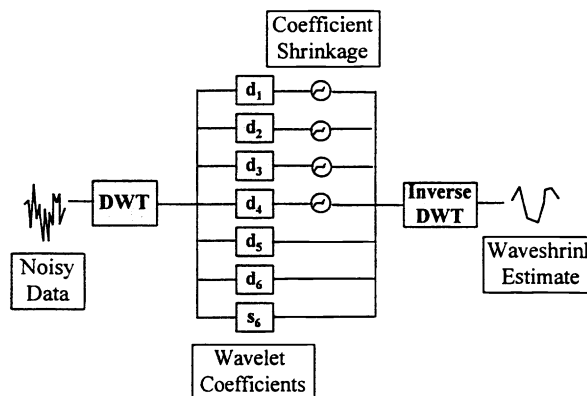


Figure 8. The wavelet shrinkage algorithm

For certain values of λ_j , the wavelet shrinkage estimate has been shown to nearly achieve the minimax risk over a broad class of functions.¹⁰ This means that it gives nearly the best possible estimate of the unknown function while making minimal assumptions about it. In particular, it does not assume that the unknown function is smooth. Wavelet shrinkage also has a locally adaptive bandwidth, in the sense that for smooth parts of the signal the estimate uses larger bands of data, and for irregular parts it uses smaller bands. It therefore works well on temporarily/spatially inhomogeneous signals, for example nonstationary random ones. The algorithm is also largely automatic, having relatively little dependence on tuning parameters.

For our experiments, we choose a soft shrinkage function $\delta_{\lambda\sigma}$. It is based on the principle that the noise affects all coefficients, even the larger ones. The shrinkage function is

$$\delta_{\lambda\sigma}(x) = \begin{cases} 0 & \text{if } |x| \leq \lambda\sigma \\ \text{sign}(x)(|x| - \lambda\sigma) & \text{if } |x| > \lambda\sigma. \end{cases} \quad (21)$$

This function is shown in Figure 9.

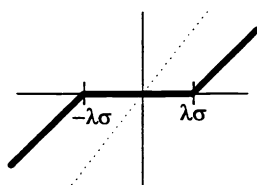


Figure 9. Wavelet coefficient shrinkage function

We use a universal threshold⁴ $\lambda_j = \sqrt{2 \log(n)}$ for all resolution levels, where n is the number of data samples. Other rules exist for threshold values^{4,5} but the universal one yields the largest amount of shrinkage and hence smoother estimates. At each resolution level, a separate estimate is computed for the scale of the noise σ , that is $\sigma_j = \hat{\sigma}(d_j)$. The function $\hat{\sigma}$ for estimating noise scale is the median absolute deviation,¹⁵ a robust estimate of scale.

We now apply wavelet shrinkage to a signal comprised of several singularities of various widths. Figure 10 shows the discrete wavelet transform for both the source and noisy signals. Note that the source signal is represented by few wavelet coefficients, while the noise affects all of them. Figure 11 shows the discrete wavelet transform of the waveshrink estimate of the source signal. Note that the estimate is good, though some of the smaller scale coefficients have been overly shrunk. Figure 11 also shows bar plots of the energy at each wavelet scale, divided into wavelet shrinkage estimate and residual.

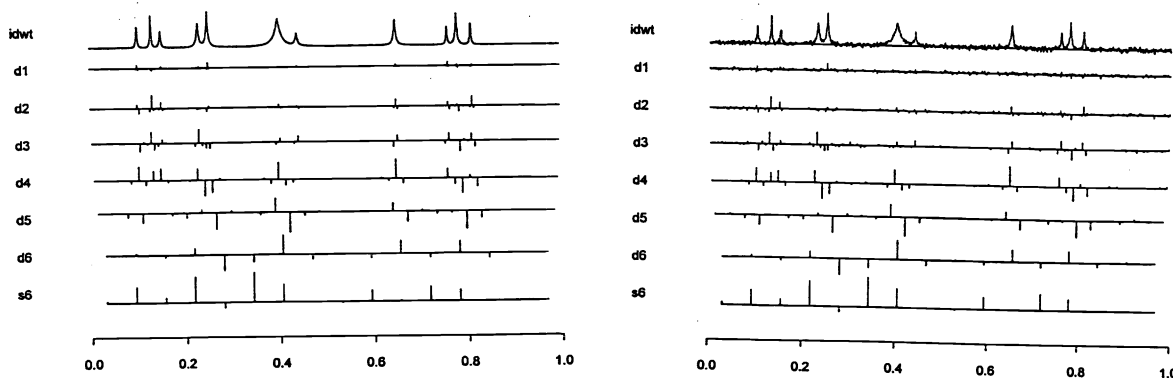


Figure 10. Discrete wavelet transforms of source and noisy signal with multiple singularities

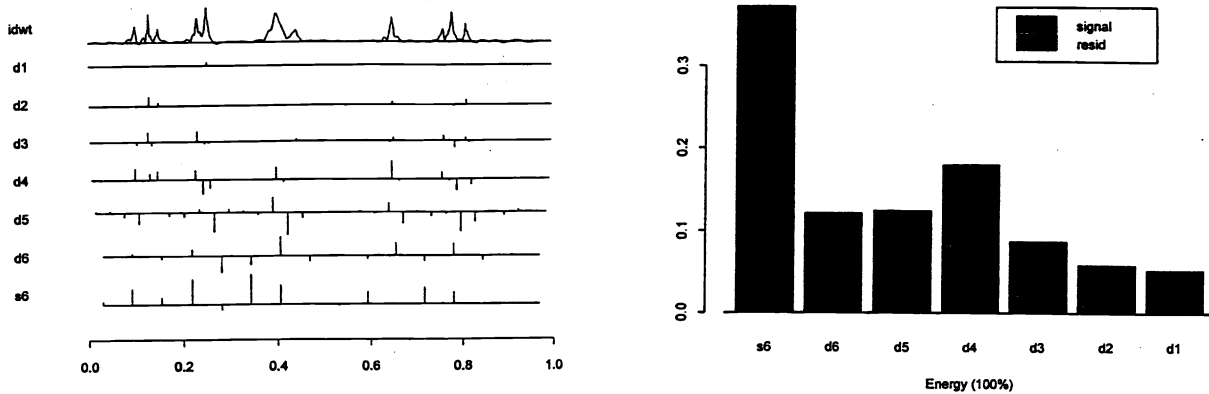


Figure 11. Discrete wavelet transform and energy plot for wavelet shrinkage estimate of source signal

4. SINGULARITY DETECTION WITH HERMITIAN HAT WAVELETS

We will now construct the complex-valued Hermitian Hat wavelet filter. We shall see that it is composed of an even function as its real part and an odd function as its imaginary part. By tracking its complex phase, it becomes a generalization of quadrature processing that has both a joint time/scale representation and a time-localized basis. We then give the Fourier transform of the Hermitian Hat wavelet, which is real. Since its transform has no complex phase, the phase of the signal is unaltered by the filter. Finally, we apply the Hermitian Hat wavelet to the detection of signal singularities corrupted by fractal noise.

The Hermitian Hat is constructed as a filter which detects signal singularities through its complex phase. More precisely, its phase is made to be the ratio of the first and second signal derivatives:

$$\theta = \tan^{-1} \left(\frac{ds/d\tau}{-d^2s/d\tau^2} \right). \quad (22)$$

Here $\theta = \theta(\tau)$ is the filter output phase, $s = s(\tau)$ is the input signal, and $\tau = \omega_0 t$ is dimensionless time, where scale frequency $\omega_0 = 2\pi/a$. The Hermitian Hat wavelet is based on the principle that in the presence of noise the differentiation should be done through filtering rather than directly. It employs dummy convolutions with the Dirac delta function $\delta = \delta(\tau)$ to accomplish this, that is

$$ds/d\tau = \delta * (ds/d\tau) = -(d\delta/d\tau) * s \quad (23a)$$

$$d^2s/d\tau^2 = \delta * (d^2s/d\tau^2) = (d^2\delta/d\tau^2) * s. \quad (23b)$$

Substituting (23a) and (23b) into (22), we have

$$\theta = \tan^{-1} \left[\frac{-(d\delta/d\tau) * s}{-(d^2\delta/d\tau^2) * s} \right]. \quad (24)$$

Note that (24) can be written in terms of filters $h_1 = -d\delta/d\tau$ and $h_2 = -d^2\delta/d\tau^2$ as

$$\theta = \tan^{-1} \left(\frac{h_1 * s}{h_2 * s} \right). \quad (25)$$

We now need to determine the form of the filters h_1 and h_2 . We begin with the Schwartz definition of $\delta(t)$ as a unit-area Gaussian function of vanishing width:

$$\delta(t) = \lim_{\omega_0 \rightarrow \infty} (1/2\pi)^{1/2} \omega_0 e^{-(\omega_0 t)^2/2}. \quad (26)$$

Taking first and second derivatives of $\delta(t)$ yields

$$h_1 = -d\delta/dt = (1/2\pi)^{1/2} \omega_0^3 t e^{-(\omega_0 t)^2/2} \quad (27a)$$

$$h_2 = -d^2\delta/dt^2 = (1/2\pi)^{1/2} \omega_0^2 [1 - (\omega_0 t)^2] e^{-(\omega_0 t)^2/2}. \quad (27b)$$

The constant term $(1/2\pi)^{1/2} \omega_0^2$ divides out of (25), so that h_1 and h_2 become dimensionless. Since h_1 is odd we denote it $h_o = h_o(\tau)$, and since h_2 is even we denote it $h_e = h_e(\tau)$, that is

$$h_o = h_1 = \tau e^{-\tau^2/2} \tag{28a}$$

$$h_e = h_2 = [1 - \tau^2] e^{-\tau^2/2} \tag{28b}$$

These 2 functions are shown in Figure 12. Note that h_e is the familiar ‘‘Mexican Hat’’ wavelet.

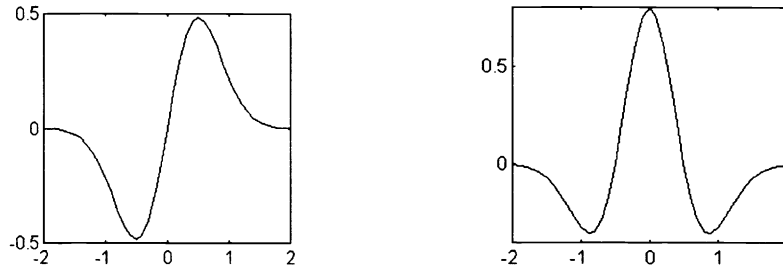


Figure 12. Hermitian Hat odd (imaginary part) and even (real part) filters

Replacing h_1 with h_o and h_2 with h_e in (25) we have

$$\theta = \tan^{-1} \left(\frac{h_o * s}{h_e * s} \right) \tag{29}$$

Thus our desired complex-valued filter is

$$h(\tau) = h_e(\tau) + j h_o(\tau) \tag{30}$$

This has been shown to be an admissible wavelet.¹ Moreover, it is a Hermitian operator, since it has the property of time reversal under complex conjugacy, that is $h^*(\tau) = h(-\tau)$. It has been named the Hermitian Hat wavelet.¹

It is of interest to compare the new Hermitian Hat wavelet with the only other complex-valued wavelet, the Morlet. Consider multiplying $h_o(\tau)$ by some real number α , that is

$$h(\tau) = h_e(\tau) + j\alpha h_o(\tau) = (1 + j\alpha\tau - \tau^2) e^{-\tau^2/2} \tag{31}$$

Also recall that

$$e^{j\alpha\tau} \approx 1 + j\alpha\tau - \alpha^2\tau^2/2 \tag{32}$$

If it were the case that $\alpha = \sqrt{2}$, then we could say that

$$h(\tau) \approx e^{j\sqrt{2}\tau} e^{-\tau^2/2} \tag{33}$$

which is the form of the Morlet wavelet. However, we would need $\alpha > 6$ for the Morlet so that its Fourier transform would nearly vanish at zero. Thus we see that while the Hermitian Hat is somewhat similar to the Morlet, they are still quite different.

The Fourier transform $H(\Omega)$ of $h(\tau)$ is

$$H(\Omega) = (\Omega^2 - \Omega) e^{-\Omega^2/2} \tag{34}$$

where $\Omega = \omega/\omega_0$. The transform is real, which is another property of Hermitian operators. Since the Fourier transform has no complex phase, the Hermitian Hat wavelet does not affect the phase of the signal. Also, $H(0) = 0$, so that it has no constant component. The Hermitian Hat accomplishes this with only about one oscillation within a Gaussian window, as opposed to about 6 for the Morlet. It is worth noting here that the Hermitian Hat is an analytical continuation of the real-valued Mexican Hat to the complex domain. This is precisely what gives the Hermitian Hat the ability to detect singularities.

We now apply the Hermitian Hat wavelet to the detection of a signal singularity corrupted by fractal noise. The signal is

$$s[t] = s_0 e^{-|t-t_0|/\tau} \tag{35}$$

where $1 \leq t \leq 256$, signal height $s_0 = 10$, signal shift $t_0 = 128$, and e-folding length $\tau = 10$. Both the source and noisy signal are shown in Figure 13.

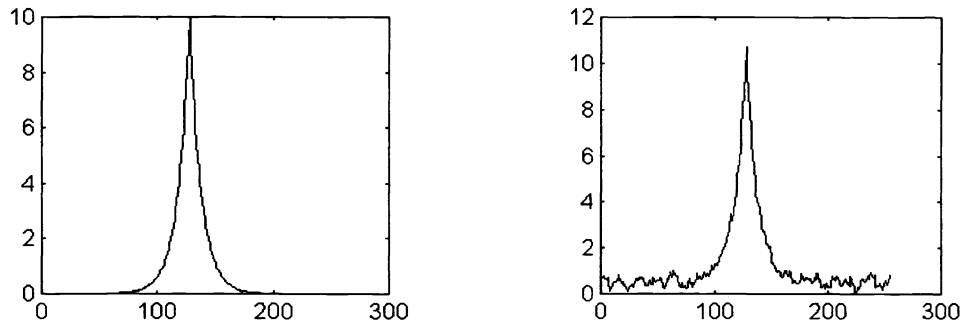


Figure 13: Source and noisy signals for wavelet detection

Figure 14 shows the real and imaginary parts of the Hermitian Hat wavelet filter output for the noisy signal. The axes from 0 to 200 are time, and those from 0 to 20 are resolution. Figure 15 shows the resulting filter output phase. A threshold of 0.1 was then applied to the phase to separate the signal singularity from the noise. The result is also shown in Figure 15.

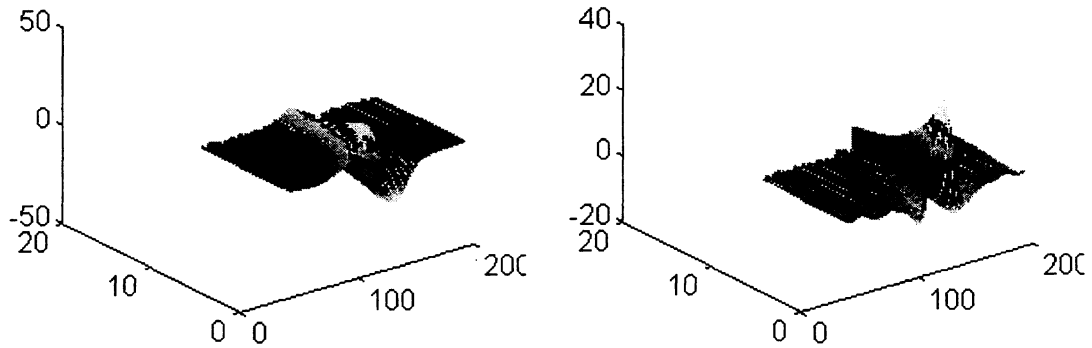


Figure 14: Real and imaginary parts of wavelet filter output

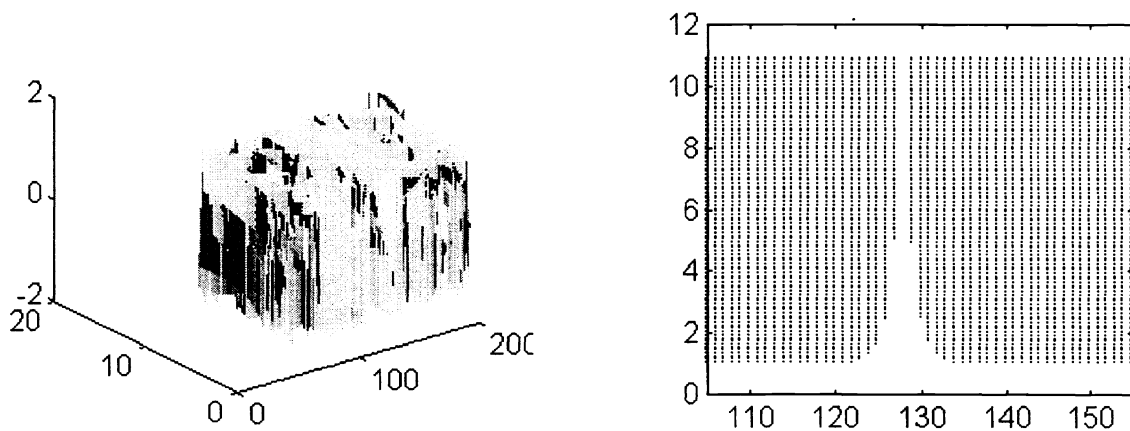


Figure 15: Phase of wavelet filter output before and after threshold

5. CONCLUSIONS AND REMARKS

In this paper we have generalized radar quadrature processing using the complex phase of the new Hermitian Hat wavelet. Because the generalization is wavelet-based, it has a joint time/scale representation and a time-localized basis. We have shown how the Hermitian Hat is constructed so as to detect signal singularities through phase bifurcations. It is like the Morlet wavelet in this sense. However, the Hermitian Hat has a narrower bandwidth than the Morlet, so that it causes less signal smearing. As its name implies, it is a Hermitian operator, so that the phase of the wavelet does not interfere with the phase of the signal. We have demonstrated computationally how the Hermitian Hat detects singularities at various scales in the presence of fractal noise. To do this we have developed a wavelet-based model which is a variation of $1/f$ fractal noise. We have also investigated how wavelet shrinkage can reduce and smooth noise before we apply Hermitian Hat detection.

ACKNOWLEDGMENTS

We gratefully acknowledge the tremendous efforts of Margaret Cleven in preparing this manuscript. We are also grateful for her ongoing dedication and support. We also thank Charles Hsu for his assistance in the computational experiments.

REFERENCES

1. H. Szu, C. Hsu, L. D. Sa, W. Li, "Hermitian Hat wavelet design for singularities detection in Paraguay river level data analyses," *Proc. SPIE Wavelet Apps. IV* (Orlando, FL), Vol. 3078, Apr. 1997.
2. R. Murenzi, *Wavelets*, eds. J. Combes, A. Grossman, P. Tchmitchian, Springer Berlin, 1988.
3. Source for (multi)fractal nature of ocean surface taken from ONR Ocean Conf., England, 1992.
4. D. Donoho, I. Johnstone, "Adapting to unknown smoothness via wavelet shrinkage," Technical report, Dept. of Statistics, Stanford Univ., 1992.
5. D. Donoho, I. Johnstone, "Ideal spatial adaptation via wavelet shrinkage," Technical report, Dept. of Statistics, Stanford Univ., 1992.
6. D. Donoho, I. Johnstone, "Minimax estimation via wavelet shrinkage," Technical report 402, Stanford Univ., 1992.
7. D. Donoho, "Nonlinear wavelet methods for recovery of signals, densities, and spectra from indirect and noisy data," *Proc. Symp. Appl. Math.*, AMS, 1993.
8. D. Donoho, "De-noising by soft thresholding," *IEEE Trans. Sig. Proc.*, 1994.
9. S. Mallat, "A theory for multiresolution signal decomposition: The wavelet representation," *IEEE Trans. Patt. Anal. Mach. Intell.*, Vol. II, No. 7, pp. 674-693, 1989.
10. B. Mandelbrot, *Fractal Geometry of Nature*, Freeman, 1983.
11. J. Feder, *Fractals*, Plenum, 1988.
12. G. Wornell, *Signal Processing With Fractals: A Wavelet-Based Approach*, Prentice Hall, 1996.
13. I. Daubechies, *Ten Lectures on Wavelets*, SIAM, Philadelphia, 1992.
14. H. Leung, S. Haykin, "Is there a radar clutter attractor?," *Appl. Phys. Lett.* **56**(6), 1990.
15. W. Venables, B. Ripley, *Modern Applied Statistics With S-Plus*, Springer-Verlag, 1994.